# Effects of competing orders and quantum criticality on the quasiparticle tunneling spectroscopy and vortex dynamics of cuprate superconductors

N.-C. Yeh[a], C.-T. Chen[a], C. R. Hughes[a], A. D. Beyer[a], V. S. Zapf[b], and S. I. Lee[c]
[a]Department of Physics, California Institute of Technology, Pasadena, CA 91125, USA
[b]National High Magnetic Field Laboratory, Los Alamos National Laboratory, Los Alamos, NM
[c]Department of Physics, Pohang University of Science and Technology, Pohang 790-784, Korea

## ABSTRACT

The effect of competing orders and quantum criticality on the macroscopic vortex dynamics and microscopic low-energy excitations of cuprate superconductors is investigated using high-field magnetic measurements and low-temperature scanning tunneling spectroscopy. Our experimental results suggest that significant field-induced quantum fluctuations at low temperatures are present in all cuprates investigated, suggesting that cuprate superconductors are in close proximity to a quantum critical point (QCP) that separates a pure superconducting phase (SC) from a phase consisting of coexisting SC and a competing order. The proximity of a cuprate to the QCP can be determined from a normalized characteristic field in the zero-temperature limit, and the characteristic field correlates well with the quasiparticle tunneling spectra, showing increasing spectral deviation from the mean-field behavior for samples of closer proximity to the QCP. Macroscopically, the presence of competing order can induce strong fluctuation effects in the cuprate superconductors, which is consistent with the extreme type-II nature of the cuprates. The relevant competing orders in different cuprates are examined by comparing theory with experimental data, and the physics implications of these studies are discussed.

**Keywords:** competing orders; quantum criticality; quantum fluctuations; quasiparticle tunneling spectroscopy; vortex dynamics.

## 1. INTRODUCTION

Cuprate superconductors are extreme type-II superconductors that exhibit strong thermal, disorder and quantum fluctuations in the vortex states[1-6]. While much research has focused on the *macroscopic* vortex dynamics of cuprate superconductors with theoretical descriptions at a phenomenological level using the London or Landau-Ginzburg theory[1-3], as exemplified in Fig. 1(a)-(b) for the theoretical magnetic field ($H$) versus temperature ($T$) vortex phase diagrams, little effort has been made to address possible physical origin of their extreme type-II nature. *Microscopically*, cuprate superconductors differ fundamentally from conventional superconductors in that they are doped Mott insulators with strong electronic correlation that gives rise to different thermodynamic phases, known as competing orders (CO), in the ground state besides superconductivity (SC).[7-12] The existence of competing orders and the proximity to quantum criticality have significant consequences on the overall low-energy excitation spectra of the cuprates, because low-energy excitations of competing orders can complicate the Bogoliubov quasiparticle spectrum of superconductivity, leading to such unconventional phenomena[11] as quasiparticle spectral modulations[13-20] and dichotomy in the quasiparticle coherence[18,21-25] of the underdoped hole-type cuprates, and the excess low-energy density of states (DOS) in the electron-type cuprates of varying doping levels[26-29]. Moreover, competing orders are likely responsible for various non-universal phenomena in the cuprates,[21-23] including the pairing symmetry[28,30-41], pseudogap[26-29,42-44], spatial homogeneity of the quasiparticle tunneling spectra[33-35,45-47], and commensuration of the spin excitations.[48-51]

Generally speaking, the interplay between CO and SC and the resulting phase diagrams are dependent on the material parameters (*e.g.* the doping level, onsite Coulomb repulsion, pairing strength, interlayer superconducting coupling strength, degree of disorder), and on external variables such as the temperature ($T$) and applied magnetic field ($H$), as exemplified in Fig. 2(a)-(b) for the $T$-vs.-$\alpha$ and $H$-vs.-$\alpha$ phase diagrams, where $\alpha$ denotes a representative material parameter. Thus, cuprate superconductors exhibit strong susceptibility to increasing temperature, magnetic field and

disorder, and we suggest that their extreme type-II nature and the manifestation of strong thermal, disorder and quantum fluctuations may be attributed in part to the presence of competing orders and their proximity to quantum criticality.[52-54]

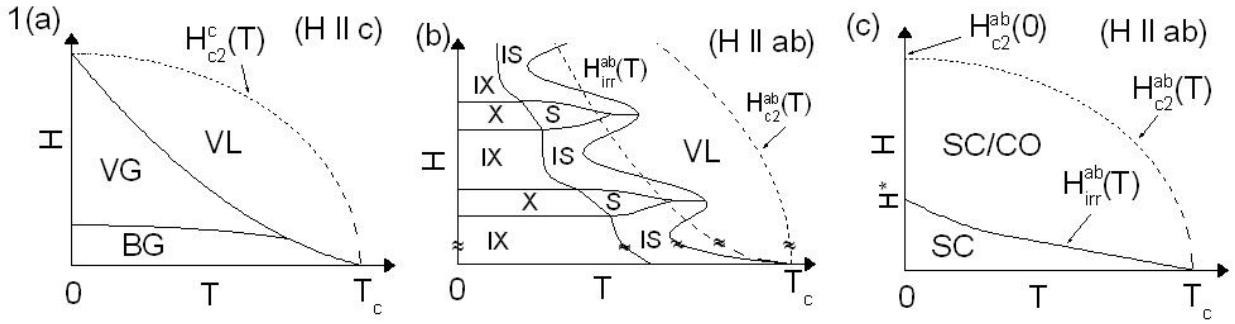


**Fig. 1** Schematic vortex phase diagrams for cuprate superconductors: **(a)** The *H*-vs.-*T* phase diagram for applied magnetic field perpendicular to the $CuO_2$ planes ($H \parallel c$-axis),[4] assuming thermal fluctuations and relevant random point disorder. Neglecting the lower critical field $H_{c1}$ due to the extreme type-II nature, we find the vortex phase with increasing *H* and *T* evolves from the Bragg glass (BG) to the vortex glass (VG) and then the vortex liquid (VL) before reaching the upper critical field $H_{c2}^{c}$. **(b)** The *H*-vs.-*T* phase diagram for applied magnetic field parallel to the $CuO_2$ planes ($H \parallel ab$),[5,6] assuming dominating *thermal* fluctuations and intrinsic pinning effects due to the periodic $CuO_2$ planes without considering quantum fluctuations. Depending on whether the vortex spacing along the c-axis is commensurate with the spacing between the $CuO_2$ planes, the phase boundary separating the commensurate vortex smectic (S) phase or the incommensurate vortex smectic (IS) phase from the vortex liquid (VL) will modulate with increasing *H*. On the other hand, at sufficiently low temperatures the vortex smectic phase can order into a commensurate vortex crystal (X) or an incommensurate vortex crystal (IX) phase in the absence of significant random disorder. In general random point disorder tends to stabilize the vortex smectic phase against the vortex liquid while turning the vortex crystal into a vortex glass. In contrast, magnetic field misalignment and stacking faults of the $CuO_2$ planes tend to smear the modulations of the S/IS to VL phase boundary and reduce the phase boundary into monotonically dependent on *H*, as schematically illustrated by the dashed curve. **(c)** The *H*-vs.-*T* phase diagram for applied magnetic field parallel to the $CuO_2$ planes ($H \parallel ab$), assuming dominating *quantum* fluctuations associated with the proximity to quantum criticality and competing orders.[52-54]

In this work, we investigate the effect of competing order and quantum criticality on the microscopic quasiparticle spectra and macroscopic vortex dynamics of various electron- and hole-type cuprate superconductors via experimental studies of the high-field thermodynamic phase diagrams and low-temperature scanning tunneling spectroscopy. To address the issue of quantum fluctuations on the vortex dynamics of cuprate superconductors, we focus on studies of the vortex phase diagram at $T \rightarrow 0$ to minimize the effect of thermal fluctuations and with magnetic field parallel to the $CuO_2$ planes ($H \parallel ab$) to minimize the effect of random point disorder fluctuations.[52-54] The rationale for the latter approach is that the intrinsic pinning effect of $CuO_2$ planes generally dominates over the pinning effects of random point disorder, and in the absence of significant quantum fluctuations, theory suggests that random point disorder cooperates with the intrinsic pinning effect and stabilizes the low-temperature vortex smectic and vortex solid phases (see Fig. 1(b)) that are true superconducting states with persist currents[5,6]. Moreover, the modulating vortex phase boundaries due to varying commensurate-to-incommensurate fields relative to the c-axis crystalline periodicity tend to be smoothed out due to slight magnetic field misalignment and/or stacking faults of the $CuO_2$ planes.[5,6] Thus, in the absence of quantum fluctuations, the vortex phase diagram for $H \parallel ab$ would resemble that of the vortex-glass and vortex-liquid phases in Fig. 1(a), as illustrated in Fig. 1(b) with the dashed line. On the other hand, if quantum fluctuations are dominant, the vortex phase diagram for $H \parallel ab$ would deviate substantially from the prediction solely based on thermal fluctuations and intrinsic pinning, and we expect suppression of the truly superconducting phase (i.e. the phase with non-dissipative persistent currents) at $T \rightarrow 0$, as illustrated in Fig. 1(c). We shall demonstrate in the following that our experimental results are consistent with the notion that all cuprate superconductors exhibit significant field-induced quantum fluctuations as manifested by a characteristic field $H^*(\alpha) << H_{c2}^{ab}(T=0,\alpha)$, and the degree of quantum fluctuations determined from the macroscopic magnetic measurements correlates well with the microscopic quasiparticle spectra, with increasing spectral deviation from the mean-field behavior for samples of smaller values of $h^*(\alpha) \equiv [H^*/H_{c2}^{ab}(0,\alpha)]$ that indicate closer proximity to quantum criticality and stronger quantum fluctuations. Here $H_{c2}^{ab}(0,\alpha)$ denotes the zero-temperature upper critical field (for $H \parallel ab$) for a cuprate with a material parameter $\alpha$. This finding implies close proximity of the cuprates to a quantum critical point (QCP) that separates a pure superconducting (SC) state from a

coexisting state of SC and a competing order. We also examine the nature of the relevant competing orders in the context of existing experimental evidence and theory, and suggest that charge-density wave (CDW) is likely the relevant competing order in the electron-type cuprates of *s*-wave pairing symmetry, whereas spin-density wave (SDW) seems more favorable for the hole-type cuprates, although we caution that the occurrence of SDW and CDW is often hand-in-hand in many cuprates.

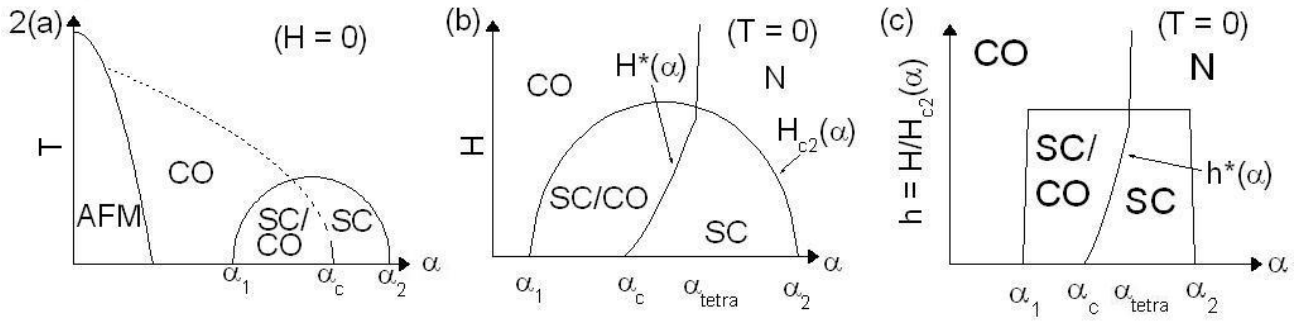


**Fig. 2** Schematic phase diagrams for cuprate superconductors: **(a)** $T$-vs.-$\alpha$ at $H = 0$;[12] **(b)** $H$-vs.-$\alpha$ at $T = 0$,[55] where $\alpha$ denotes one of the relevant material parameters such as the doping level, onsite Coulomb repulsion, pairing potential, number of $CuO_2$ layers per unit cell, and disorder; and **(c)** reduced field $h \equiv H/H_{c2}(\alpha)$ vs. $\alpha$ at $T = 0$. The field-dependence of the antiferromagnetic (AFM) phase is not explicitly shown in (b). SC: superconductivity; CO: competing order; N: normal state; $T_c$: superconducting transition temperature; $T^*$: pseudogap temperature; $T_N$: Néel temperature of the AFM phase transition; $H_{c2}$: upper critical field; $H^*$: characteristic field that separates pure SC from coexisting SC/CO; $\alpha_i$ ($i$ = 1, 2, $c$): quantum critical points; and $\alpha_{tetra}$: tetracritical point. Note that $\alpha_1 < \alpha_c < \alpha_{tetra} < \alpha_2$, and that the SC phase for $\alpha_c < \alpha < \alpha_{tetra}$ may consist of a coexisting fluctuating CO if the CO is one of the unconventional density waves such as SDW[7-9,55], CDW[12], and d-density wave (DDW)[10]. In the event that the competing order is SDW, $H^*(\alpha)$ has been determined for $\alpha \rightarrow \alpha_c^+$ by the relation $H^*(\alpha)/H_{c2}^{max} \propto (\alpha-\alpha_c)/\ln[1/(\alpha-\alpha_c)]$, where $H_{c2}^{max} \equiv H_{c2}^{ab}(\alpha_{tetra})$.[55]

## 2. EXPERIMENTAL STUDIES OF THE COMPETING ORDERS & QUANTUM FLUCTUATIONS

To investigate the relevance of competing orders and quantum criticality to the macroscopic vortex dynamics and microscopic quasiparticle spectra of cuprate superconductors, we employ various magnetic measurement techniques to determine the magnetic irreversibility field $H_{irr}(T)$ and the upper critical field $H_{c2}(T)$, and also perform low-temperature scanning tunneling spectroscopy to compare the low-energy excitations of cuprates with different values of a normalized characteristic field $h^* \equiv [H^*/H_{c2}^{ab}(0)]$ that characterizes the degree of quantum fluctuations in each sample. Here the characteristic field $H^*$ is defined as $H^* \equiv H_{irr}^{ab}(T\rightarrow 0)$, and $H_{c2}^{ab}(0) \equiv H_{c2}^{ab}(T\rightarrow 0)$, with $H_{c2}^{ab}$ being the upper critical field for $H \parallel ab$. In the event that $H_{c2}^{ab}(0)$ exceeds the paramagnetic field $H_p \equiv \Delta_{SC}(0)/(2^{1/2}\mu_B)$ for highly anisotropic cuprates, where $\Delta_{SC}(0)$ denotes the superconducting gap at $T = 0$, the characteristic field is defined as $h^* \equiv (H^*/H_p)$ because $H_p$ becomes the maximum critical field for superconductivity. The rationale for using the value of $h^*$ to characterize the degree of quantum fluctuations is based on the conjecture that strong quantum fluctuations between the field-induced CO and SC can lead to reduced phase stiffness for the SC state whenever the applied magnetic field exceeds $H^*$, provided that the relevant material parameter $\alpha$ of the sample satisfies the condition $\alpha_c < \alpha < \alpha_{tetra}$. Thus, we expect that samples with $h^* \rightarrow 0$ reveal strong quantum fluctuations and significant deviation from mean-field behavior, whereas samples with $h^* \rightarrow 1$ should be reasonably well described by the mean-field theory of superconductivity.

Specifically, the experimental results obtained from our measurements consist of studies on the electron-type optimally doped infinite-layer cuprate $La_{0.1}Sr_{0.9}CuO_2$ (La-112, $T_c$ = 43 K)[28,54] and one-layer $Nd_{1.85}Ce_{0.15}CuO_{4-\delta}$ (NCCO, $T_c$ = 21 K)[56]; and the hole-type optimally doped $HgBa_2Ca_3Cu_4O_x$ (Hg-1234, $T_c$ = 125 K), $HgBa_2Ca_4Cu_5O_x$ (Hg-1245, $T_c$ = 110 K), and $YBa_2Cu_3O_{7-\delta}$ (Y-123, $T_c$ = 93 K)[57]. Results obtained by other groups on hole-type underdoped Y-123 ($T_c$ = 87 K)[58], over- and optimally doped $Bi_2Sr_2CaCu_2O_{8+x}$ (Bi-2212, $T_c$ = 60 K and 93 K)[59,60]; and electron-type optimally doped $Pr_{1.85}Ce_{0.15}CuO_{4-\delta}$ (PCCO, $T_c$ = 21 K)[43], are also analyzed and tabulated in Table 1 for comparison. The optimally doped samples of La-112, Hg-1234 and Hg-1245 were prepared under high pressures, with details of the synthesis and characterizations described elsewhere.[61-63] We note that while the nominal doping level is generally a good representation for the average doping level of each $CuO_2$ layer in samples with one or two-layers of $CuO_2$ planes per unit

cell, it is no longer a proper indicator for the average doping level of each $CuO_2$ layer if $n \geq 3$ (with $n$ being the number of $CuO_2$ planes per unit cell) because of charge imbalance between those "outer" $CuO_2$ layers immediately adjacent to the charge reservoir and those "inner" layers farther from the charge reservoir.[64,65] The inner layers are generally underdoped regardless of the nominal doping level and thus prone to the occurrence of CO. This notion is consistent with recent NMR and neutron scattering experimental data that reveal increasing magnetic ordering possibly due to the SDW order with increasing $n$ in both the Hg- and Bi-based cuprates.[64,65] Specifically, for an averaged doping level $\delta$ of an $n$-layer cuprate, if the real doping level of an inner $CuO_2$ layer is $x\delta$ with $0 < x < 1$, the doping level of an outer $CuO_2$ layer becomes $[1-(n-2)x]\delta/2$.[64]

### 2.1 Measurements of Macroscopic Vortex Dynamics

The upper critical field $H_{c2}(T)$ was determined by measurements of the magnetic penetration depth in pulsed fields up to 65 Tesla, and $H_{c2}^0 \equiv H_{c2}(T \rightarrow 0)$ was extrapolated from $H_{c2}(T)$ values determined at finite temperatures. The experiments involved measuring the frequency shift $\Delta f$ of a tunnel diode oscillator (TDO) resonant tank circuit with the sample contained in one of the component inductors.[66] Small changes in the resonant frequency can be related to changes in the penetration depth $\Delta\lambda$ by $\Delta\lambda = -(R^2/r_s)(\Delta f/f_0)$, where $R$ is the radius of the coil, $r_s$ is the radius of the sample, and $f_0$ is the resonant frequency of the TDO for samples in the normal state.[66] In our case, $R \sim r_s = 0.7$ mm and the reference frequency $f_0 \sim 60$ MHz such that $\Delta f \sim (0.16\ \text{MHz}/\mu\text{m})\Delta\lambda$. Further details of the pulsed-field measurements can be found in Ref. 54, and representative data of the TDO measurements for La-112 is shown in Fig. 3(a).

The magnetization $M(T,H)$ measurements were conducted using several different experimental techniques. Specifically, for lower DC fields a Quantum Design SQUID magnetometer for $H$ up to 5 Tesla and a homemade Hall probe magnetometer for $H$ up to 9 Tesla at Caltech were employed. For higher DC fields (up to 33 Tesla in a $^3$He refrigerator) a cantilever magnetometer at the National High Magnetic Field Laboratory (NHMFL) in Tallahassee was used for the magnetization measurements. For even higher magnetic fields (up to 50 Tesla in a $^3$He refrigerator), a compensated coil in the pulsed-field facilities at the NHMFL in Los Alamos was used to determine the magnetization.[54] Consistency between $M(T,H)$ determined with DC field techniques and those obtained from pulsed-field facilities was also carefully verified in two systems La-112 and Hg-1234. The irreversibility field $H_{irr}(T)$ was identified from the onset of reversibility in the $M(T,H)$ loops, as exemplified in the main panel of Fig. 3(b) for pulsed-field measurements of the La-112 sample, and in the inset of Fig. 3(b) for SQUID measurements of the Hg-1245. Similar $M(T,H)$ loops of the Hg-1234 sample determined with the cantilever technique are shown in Fig. 3(c). The guiding principle of all cantilever magnetometry is to detect the deflection of a flexible beam on which a magnetic sample is mounted in response to an external quasi-static magnetic field.[67,68] For our experiments, the metallic flexible beam was coupled to a capacitance bridge so that deflection of the beam due to the sample response to an applied field was determined as the changes in the capacitance. More details for the cantilever magnetometry and calibrations can be found in Refs. 67 and 68. Representative results of the $H$-vs.-$T$ phase diagrams ($H \parallel ab$) for La-112 and Hg-1234 thus obtained are shown respectively in the main panel and the inset of Fig. 3(d), which clearly demonstrate the strong suppression of $H^*$ relative to $H_{c2}^{ab}(0) \sim H_p$, consistent with the notion of strong quantum fluctuations.

In addition to the aforementioned methods of magnetization measurements, another technique using the Hall probe magnetometry to determine the third-harmonic magnetic susceptibility $\chi_3$ was also employed to determine some of the $H_{irr}(T)$ data of Hg-1234 and Y-123 samples, as specified in our papers previously.[52,53] A collection of measured $H_{irr}(T)$ and $H_{c2}(T)$ curves for four different cuprates Y-123, La-112, Hg-1234 and Hg-1245 are summarized in Fig. 3(e), with the reduced characteristic fields $h^*$ explicitly given. We note that the Hg-1234 and Hg-1245 samples, while having the highest $T_c$ values (125 K and 110 K) and upper critical fields ($H_p \sim H_{c2}^{ab}(0) \sim 370$ Tesla and $\sim 320$ Tesla), have the most suppressed irreversibility lines and the smallest $h^*$ values. The fact that $H_{irr}^{ab}(T) << H_{c2}^{ab}(T)$ in Hg-1234 and Hg-1245 for all temperatures except very near $T_c$ can be attributed to both their extreme two-dimensionality (2D)[62,63] that leads to strong thermal fluctuations at high temperatures and their close proximity to quantum criticality that leads to strong quantum fluctuations at low temperatures. The latter assertion is corroborated by the empirical findings from muon spin resonance ($\mu$SR) and Knight shift measurements that the carrier distribution among the $CuO_2$ multi-layers within each unit cell is inhomogeneous[64,65], with the inner $CuO_2$ layers being generally underdoped, so that the larger number of inner layers there are in a cuprate superconductor, the stronger tendency it is to induce CO and to reveal more significant quantum fluctuations at low temperatures. This scenario is consistent with our finding that $h^*$(Hg-1245) $\sim 0.05 <<$

$h^*$(Hg-1234) ~ 0.20. The $h^*$ values of various cuprates investigated in the work and those obtained from literature by other research groups are summarized in Table 1.

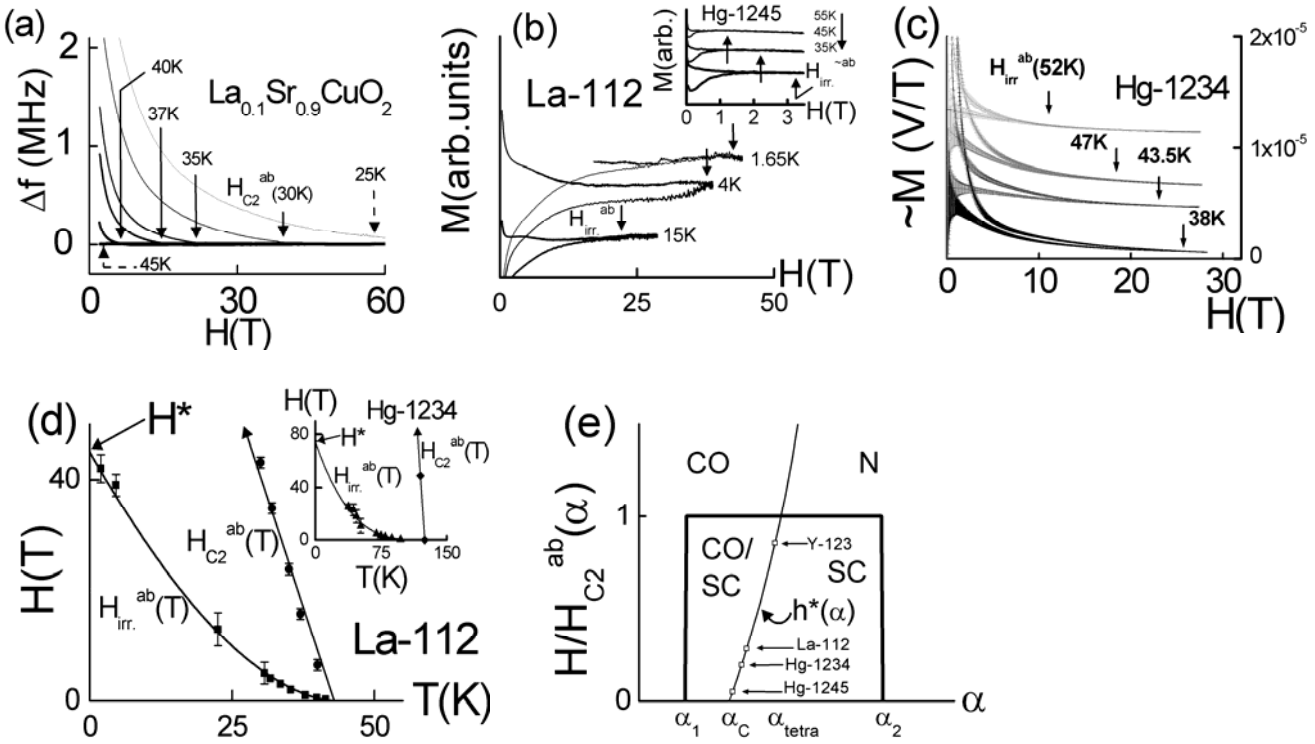


**Fig. 3** Macroscopic measurements of the upper critical field $H_{c2}^{ab}(T)$ and irreversibility field $H_{irr}^{ab}(T)$ of various cuprates: **(a)** The $H_{c2}^{ab}(T)$ of a La-112 sample is determined by measuring the resonant frequency shift $\Delta f$ of the tunnel diode oscillator as a function of $H$ for a given $T$. **(b)** The $H_{irr}^{ab}(T)$ of a La-112 sample (main panel) and that of a Hg-1245 sample (inset) are determined by measuring the magnetization loops using an inductive coil technique and a SQUID magnetometer, respectively. **(c)** The $H_{irr}^{ab}(T)$ of a Hg-1234 sample is determined by measuring the magnetization data (in arbitrary units) using the capacitive cantilever magnetometry. **(d)** The vortex phase diagrams of electron-type La-112 (main panel) and hole-type Hg-1234 (inset) for $H \parallel ab$, showing significant suppression of $H_{irr}^{ab}(T)$ relative to $H_{c2}^{ab}(T)$ in both samples. Comparison of these results with Fig. 1 suggests that substantial quantum fluctuations are present. **(e)** Normalized characteristic fields $h^*(\alpha) = [H^*/H_{c2}^{ab}(T=0,\alpha)]$ for Y-123, La-112, Hg-1234 and Hg-1245.

### 2.2 Measurements of Microscopic Quasiparticle Tunneling Spectroscopy

Our conjecture that a small normalized characteristic field $h^*$ of a cuprate superconductor corresponds to strong quantum fluctuations and close proximity to a QCP $\alpha_c$ can be further verified by studying the microscopic quasiparticle tunneling spectroscopy taken with a low-temperature scanning tunneling microscope. Specifically, we compare two types of spectral characteristics. One is the temperature evolution of the SC energy gap $\Delta_{SC}(T)$ with $h^*$, and the other is the extent of the spectral deviation from mean-field behavior with varying $h^*$. In the case of variations of $\Delta_{SC}(T)$ with $T$ and $h^*$, we compare optimally doped electron-type cuprates La-112 ($h^*$ ~ 0.28) and PCCO ($h^*$ ~ 0.53), and find that with increasing $T$, the rate of decrease in $\Delta_{SC}(T)$ of the La-112 sample is significantly faster than that of the PCCO sample, consistent with the notion that La-112 is much closer to the QCP $\alpha_c$ because of a significantly smaller $h^*$, as detailed in Ref. 52. The other spectral verification for our conjecture can be found in the quasiparticle tunneling spectra exemplified in Fig. 4(a)-(b) for the comparison of optimally doped cuprates of La-112 ($h^*$ ~ 0.28) and Y-123 ($h^*$ ~ 0.85). In the case of electron-type La-112, the quasiparticle spectra of La-112 are momentum-independent and its response to quantum impurities is consistent with *s*-wave pairing.[28] However, the low-energy spectral characteristics deviate significantly from the mean-field theory for *s*-wave superconductors, with excess sub-gap (i.e., quasiparticle energies $|E| < \Delta_{SC}$) spectral weight suggestive of excess low-energy excitations that cannot be reconciled with simple quasiparticle excitations from a pure SC state.[26-28,52,53] In contrast, the low-energy (up to $|E| \sim \Delta_{SC}$) directional quasiparticle tunneling

spectra on Y-123 can be well accounted for by the mean-field generalized BTK model for *d*-wave superconductors,[32-35] as exemplified in Fig. 4(b) for the c-axis tunneling spectrum of an optimally doped Y-123. While the spectral satellite features at $|E| > \Delta_{SC}$ have been attributed to quasiparticle interaction with bosonic excitations such as the ($\pi$, $\pi$) spin resonance or incommensurate spin fluctuations,[69-71] the good spectral agreement with mean-field behavior at low energies implies that the effect of competing order is only significant at higher energies, which is consistent with the much larger $h^*$ value (~ 0.85) for Y-123 and therefore much weaker quantum fluctuations.

**Table 1** Comparison of the values of the normalized characteristic field $h^* \equiv (H^*/H_p)$ for various cuprate superconductors. Here $H_p \equiv \Delta_{SC}(0)/(2^{1/2}\mu_B)$ denotes the paramagnetic field, $H_p \sim H_{c2}{}^{ab}(0)$ for highly anisotropic cuprates with $H \parallel ab$, and $\Delta_{SC}(0)$ is the superconducting gap at $T = 0$.

| Cuprates | $T_c$ (K) | h* | Type | Doping Level | Pairing Symmetry |
|---|---|---|---|---|---|
| $La_{0.1}Sr_{0.9}CuO_2$ (La-112)[28,54] | 43 | 0.28 | electron-type | optimally doped | *s* -wave |
| $Nd_{1.85}Ce_{0.15}CuO_{4-\delta}$ (NCCO)[56] | 21 | 0.53 | electron-type | optimally doped | *s* -wave |
| $Pr_{1.85}Ce_{0.15}CuO_{4-\delta}$ (PCCO)[43] | 21 | 0.53 | electron-type | optimally doped | *s* -wave |
| $HgBa_2Ca_3Cu_4O_x$ (Hg-1234) | 125 | 0.20 | hole-type | charge imbalance | $d_{x^2-y^2}$-wave |
| $HgBa_2Ca_4Cu_5O_x$ (Hg-1245) | 110 | 0.05 | hole-type | charge imbalance | $d_{x^2-y^2}$-wave |
| $YBa_2Cu_3O_x$ (Y-123)[53,57] | 93 | 0.85 | hole-type | optimally doped | $d_{x^2-y^2}$-wave |
| $YBa_2Cu_3O_x$ (Y-123)[58] | 87 | 0.6 | hole-type | underdoped | $d_{x^2-y^2}$-wave |
| $Bi_2Sr_2CaCu_2O_x$ (Bi-2212)[59] | 60 | 0.45 | hole-type | overdoped | $d_{x^2-y^2}$-wave |

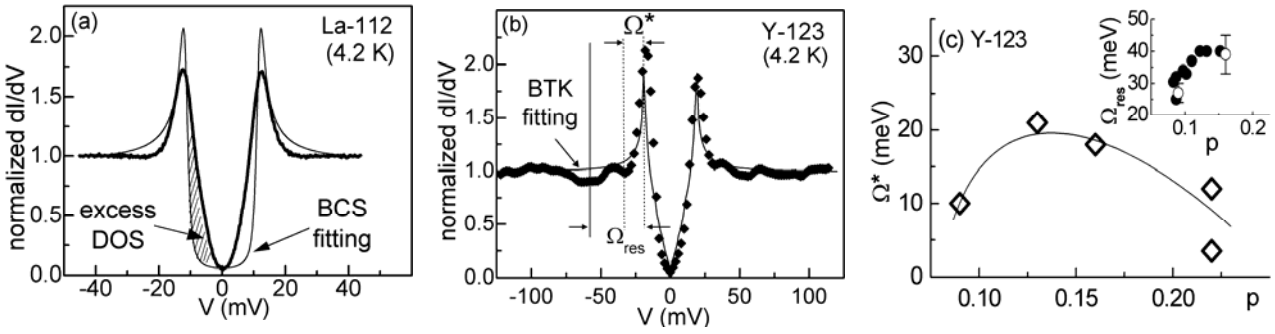


**Fig. 4** Comparison of the quasiparticle spectral characteristics for cuprates of different values of $h^*$: **(a)** Momentum-independent normalized tunneling spectrum (solid dots) of La-112 at 4.2 K, showing significant deviation from mean-field *s*-wave behavior (thin solid line) and substantial excess low-energy excitations. **(b)** Normalized tunneling spectrum (solid diamonds) of optimally doped Y-123 at 4.2 K, showing good agreement with mean-field generalized BTK model (thin solid line) for low-energy excitations up to $|E| \sim \Delta_{SC}$. The spectral satellite features at $|E| > \Delta_{SC}$ appear to correlate with quasiparticle interaction with the ($\pi$, $\pi$) spin fluctuations, and the energy of the "dip" feature can be expressed as $|E_{dip}| \sim \Delta_{SC} + \Omega_{res}$ where $\Omega_{res}$ is the resonant energy of the ($\pi$, $\pi$) spin fluctuations.[69-71] **(c)** The doping ($p$) dependence of the first dip $\Omega^* \equiv |E'_{dip}| - \Delta_{SC}$ (main panel) and that of the second dip $\Omega_{res} \equiv |E_{dip}| - \Delta_{SC}$ for Y-123 (inset, open circles) as determined from our scanning tunneling spectroscopic studies are compared with the $\Omega_{res}$ values obtained from neutron scattering experiments in the inset[48,49] (solid circles). We note that the energy scale and the doping dependence of the second dip feature in our tunneling spectra agree with the ($\pi$,$\pi$) spin resonance data from neutron scattering[48,49] although the signal to noise ratio is not as good as that for the first dip, whereas the first dip feature with the energy $\Omega^* < \Omega_{res}$ is likely associated with the incommensurate spin fluctuations in Y-123. The findings in Y-123 differ from those of Bi-2212 where quasiparticle spectra only exhibit one dip feature[60] and the corresponding neutron scattering data reveal only the ($\pi$, $\pi$) spin resonance but no incommensurate spin fluctuations.

### 2.3 Direct Comparison of Microscopic and Macroscopic Measurements – Current-induced pseudogap phenomena in electron-doped infinite layer cuprates $Sr_{0.9}La_{0.1}CuO_2$

A further verification for the closer proximity of La-112 to quantum criticality than Y-123 is manifested in Fig. 5(a)-(b), where the quasiparticle tunneling spectra of La-112 are found to be dependent on the tunneling current $I$. For lower tunneling currents, we find that the coherence peaks at $E = \pm\Delta_{SC}$ are systematically suppressed with increasing $I$ without changing the $\Delta_{SC}$ value for $I < I^* \sim 20 \pm 5$ μA. For $I > I^*$ additional hump-like spectral features begin to emerge at higher energies $|E| = \Delta_{PG}$ while the subsiding coherence peaks at $|E| = \Delta_{SC}$ remain coexistent. Finally, the original coherence peaks at $|E| = \Delta_{SC}$ completely vanish at $I > I_{cr} \sim 55 \pm 5$ μA and only the pseudogap-like features at $|E| = \Delta_{PG} > \Delta_{SC}$, as illustrated in Fig. 5(a). More detailed evolution of the superconducting and pseudogap features with $I$ is summarized in Fig. 5(b). Interestingly, we find that the ratio of the two characteristic currents $(I^*/I_{cr}) \sim 0.35 \pm 0.10$ is in reasonable agreement with the normalized characteristic field $h^* = (H^*/H_p) \sim 0.28$ determined from the macroscopic measurements, suggesting that the pseudogap induced by large local tunneling currents may be associated with the relevant competing order in La-112, and that the local tunneling currents produced an effect comparable to that by applied magnetic fields. This finding can be understood by considering the induced surface magnetic field by the tunneling current, $H \sim \mu_0\lambda_{eff}(I/A_{eff})$ so that $H \sim I$, where $\lambda_{eff}$ and $A_{eff}$ denote the effective surface penetration depth and effective area of current distribution, respectively. On the other hand, for optimally doped Y-123 with $T_c \sim 93$ K and underdoped Y-123 with $T_c \sim 60$ K, no noticeable spectral variation was ever found with tunneling currents in the same range as that used for studying La-112. This finding is consistent with our conjecture that Y-123 is farther from the QCP than La-112, (see Table 1 and Fig. 3(e)), so that it is more difficult to induce competing orders with tunneling currents in Y-123.

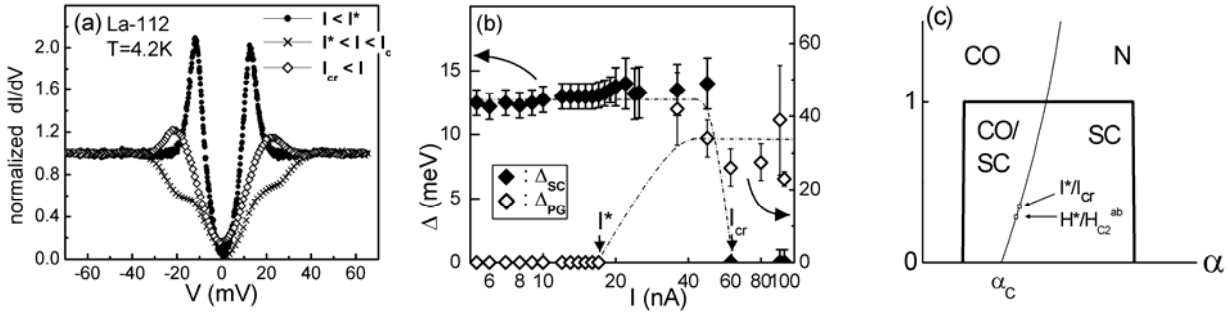


**Fig. 5** Current-induced pseudogap phenomena in La-112: **(a)** Comparison of three representative spectra taken under different tunneling currents $I < I^* \sim 20$ μA, $I^* < I < I_{cr} \sim 55$ μA, and $I > I_{cr}$. The spectrum exhibits two peaks at $E = \pm\Delta_{sc}$ for $I < I^*$, two sets of features at $E = \pm\Delta_{sc}$ and $E = \pm\Delta_{PG}$ for $I^* < I < I_{cr}$, and two peaks and $E = \pm\Delta_{PG}$ for $I > I_{cr}$. **(b)** Evolution of the superconducting gap $\Delta_{sc}$ and pseudogap $\Delta_{PG}$ with increasing tunneling currents, showing coexistence of two sets of gaps for $I^* < I < I_{cr}$. **(c)** Comparison of the ratio $(I^*/I_{cr})$ determined from scanning tunneling spectroscopy with the $h^* = [H^*/H_{c2}^{ab}(0)]$ value determined from macroscopic vortex dynamics, showing good agreement between these two distinct experiments.

## 3. DISCUSSION & THEORETICAL MODELING

Our experimental results presented in the previous section are supportive of the notion that strong field-induced quantum fluctuations exist in all cuprate superconductors due to their proximity to competing orders, and that the extreme type-II nature of cuprate superconductors may have its microscopic origin in the proximity of superconductivity to competing orders. A natural question to ask next is what the relevant competing order(s) may be and whether the competing order is universal among all cuprates. In the following we shall argue that CDW is a likely competing order for electron-doped cuprates that exhibit *s*-wave pairing symmetry, whereas the relevant competing order for hole-doped cuprates with *d*-wave pairing symmetry may be either SDW[7-9,55] or DDW[10]. We also discuss experimental and theoretical means to distinguish contributions of SDW from those of DDW.

### 3.1 CDW as the relevant competing order in electron-doped cuprates with *s*-wave pairing symmetry

The pairing symmetry in hole-type cuprate superconductors has been well established to be primarily $d_{x^2-y^2}$-wave for underdoped and optimally doped samples[30-33] and becomes ($d_{x^2-y^2}$+*s*)-wave pairing in the overdoped limit.[34-37] In contrast, the pairing symmetry of one-layer electron-type cuprates has been controversial, with different experiments suggesting either *s*-wave or $d_{x^2-y^2}$-wave pairing symmetry, or systematic evolution from $d_{x^2-y^2}$- to *s*-wave pairing with increasing electron doping.[33,39,40] Given that the undoped cuprates are Mott antiferromagnetic insulators with very large on-site Coulomb repulsion, that a large charge reservoir exists between the $CuO_2$ planes, and that the Cu atoms in each $CuO_2$ plane of all hole-type cuprates are connected to apical oxygen, it is reasonable to conjecture that the pairing symmetry favors $d_{x^2-y^2}$-wave over pure *s*-wave in most hole-type cuprates so as to minimize the on-site Coulomb repulsion while maintain the quasi-two dimensionality of the system. On the other hand, the absence of apical oxygen in electron-type cuprates results in degenerate $d_{x^2-y^2}$ and $d_{3z^2-r^2}$ orbital so that the energetic advantage of forming pure $d_{x^2-y^2}$-wave pairing is compromised, although the significantly large separation between consecutive $CuO_2$ planes in the one-layer electron-type cuprates could still favor a pairing symmetry that preserves the quasi-two dimensionality. The exact pairing symmetry in a specific sample therefore depends sensitively on the subtle balance of various competing energy scales. Furthermore, the exact doping level of electron-type cuprates is generally difficult to determine because besides the nominal doping level introduced by the cation dopants, additional procedure of oxygen reduction must be carried out to achieve superconductivity. It is the latter procedure that leads to significant uncertainties in making consistent comparison among samples prepared by different groups and even among different batches made by the same research group, particularly if the pairing symmetry is sensitively dependent on the doping level.

On the other hand, the infinite-layer n-type cuprate $Sr_{1-x}Ln_xCuO_2$ (Ln = La, Gd, Sm), known as the simplest form among all cuprate superconductors,[72-74] has several unique characteristics that differ from other cuprates and may in fact favor *s*-wave pairing. First, in contrast to all other cuprates with a large charge reservoir between the $CuO_2$ planes, the infinite-layer system only contains a metallic monolayer of La(Sr) between consecutive $CuO_2$ planes. Second, the c-axis superconducting coherence length ($\xi_c \sim 0.53$ nm) is longer than the c-axis lattice constant ($c_0$),[75] in contrast to the typical condition of $\xi_c << c_0$ in most other cuprates. Hence, the infinite-layer system is expected to reveal characteristics more like a three-dimensional superconductor.[54] Third, it is found from the Knight shift experiments[29] that the carrier density of the optimally doped $Sr_{0.9}La_{0.1}CuO_2$ (La-112) at the Fermi level is significantly smaller than that in typical p-type cuprates, being ~ 25% that of optimally doped $YBa_2Cu_3O_{7-\delta}$. These atypical characteristics of the infinite-layer system are suggestive of a stronger tendency toward more isotropic pairing symmetry as well as weaker screening and stronger electronic correlation. Indeed, our scanning tunneling spectroscopic studies have established momentum-independent quasiparticle spectra, consistent with *s*-wave pairing.[28] In addition, impurity substitution experiments[38] and vortex-state specific heat studies also led to the *s*-wave pairing scenario. However, as stated in the previous section, the low-energy excitation spectra of La-112 differ from the predictions of mean-field *s*-wave superconductivity, and the excess sub-gap low-energy excitations[28] for the quasiparticle energy range ~ 2 meV < $|E|$ < $\Delta_{sc}$ ~ 13 meV are consistent with the temperature dependent Knight shift measurements[29] that exhibit behavior comparable to *s*-wave for $T < 20$ K while more *d*-wave-like (with excitations more than those of a mean-field *s*-wave superconductor) temperature dependence at 20 K < $T < T_c$. While the aforementioned Knight shift data were attributed to *d*-wave pairing of La-112,[29] we suggest that consideration of competing orders in La-112, which was omitted in Ref. 29, is essential to account for all of the experimental findings consistently.

Specifically, it has been established both theoretically and experimentally that *s*-wave superconductivity can coexist with CDW.[76-78] Moreover, Yang and Zhang[79,80] have shown that such a system can be described by the exact symmetry of *SO*(4), and Lee[81] has further proven the duality between *s*-wave SC and CDW in two dimensions using effective field theory. The duality between these two phases implies that gapless excitations associated with the Goldstone modes can be present despite the gapped nature of both *s*-wave SC and CDW. Such quantum phase fluctuations could exist even in the absence of applied field and might account for the experimental observation of excess gapless excitations in electron-type cuprate superconductors. The coexistence of *s*-wave SC and CDW is also known to result in one type of hybridized low-energy excitations rather than two separate excitation spectra.[76,77] Therefore, long-range spectral homogeneity is expected unless significant disorder is present in the sample. Interestingly, we have indeed observed spectral homogeneity in the tunneling spectra of La-112 up to 100 nm in spatial range,[28] which is in sharp contrast to the short-range spectral variations in hole-type cuprates Bi-2212[45-47] and $Ca_{2-x}Na_xCuO_2Cl_2$ (Na-CCOC)[17].

To investigate the low-energy excitation spectra of competing *s*-wave SC and CDW, we note that theoretical studies to date have largely focused on the solutions to a mean-field Hamiltonian consisting of coexisting *s*-wave SC and static CDW, and also on the mean-field solution with added random disorder.[76,77] However, no explicit calculations have been carried out for the low-energy excitations described by the mean-field Hamiltonian plus the self-energy of the quantum phase fluctuations, the latter would be more consistent with a system of competing *s*-wave SC and dynamic CDW in the absence of applied magnetic field. Specifically, the mean-field Hamiltonian $H_{MF}$ of a system with coexisting *s*-wave SC and CDW is given by the following form:

$$H_{MF} = \sum_{\mathbf{k}\sigma}\left[\xi_{\mathbf{k}\sigma}c^{\dagger}_{\mathbf{k}\sigma}c_{\mathbf{k}\sigma} + V_0 c^{\dagger}_{\mathbf{k}+\mathbf{Q},\sigma}c_{\mathbf{k}\sigma} + V_0^{*}c^{\dagger}_{\mathbf{k}\sigma}c_{\mathbf{k}+\mathbf{Q},\sigma}\right] + \sum_{\mathbf{k}}\left(\Delta c^{\dagger}_{\mathbf{k}\uparrow}c^{\dagger}_{-\mathbf{k}\downarrow} + \Delta^{*}c_{-\mathbf{k}\downarrow}c_{\mathbf{k}\uparrow}\right), \tag{1}$$

where $\xi_{\mathbf{k}} \equiv \varepsilon_{\mathbf{k}} - \mu$ is the normal-state energy $\varepsilon_{\mathbf{k}}$ of particles relative to the chemical potential $\mu$, $\mathbf{k}$ and $\sigma$ denote the particle momentum and spin state, respectively, $\Delta$ is the SC pairing potential, $V_0$ is the CDW potential, $\mathbf{Q}$ is the CDW wave vector, and $c^{\dagger}_{\mathbf{k}}$ and $c_{\mathbf{k}}$ are the creation and annihilation operators of particles, respectively. The quasiparticle density of states $N_s(E)$ for the Hamiltonian given in EQ (1) has been shown to yield two sets of peaks at energies $E = |\Delta|$ and $E = (|\Delta|^2+|V_0|^2)^{1/2}$ without excess low-energy density of states for $E < |\Delta|$. If scattering effects due to non-magnetic impurities are added to the mean-field Hamiltonian in EQ (1), it is found that the effective superconducting pairing potential $\overline{\Delta}$ becomes enhanced by the non-magnetic impurities so that $\overline{\Delta} > \Delta$, and the density of states $N_s(E)$ still exhibit two peaks at modified energies $E = \overline{\Delta}$ and $E = \left(\overline{\Delta}^2 + V_0^2\right)^{1/2}$ without excess density of states for energies for $|E| < \overline{\Delta}$, unless magnetic impurities are added.[76,77] Hence, the mean-field Hamiltonian of coexisting *s*-wave SC and CDW, even under the present of substantial non-magnetic impurity scattering, cannot account for the significant subgap density of states in the electron-type cuprates as illustrated in Fig. 4(a).

On the other hand, effective theory of coexisting *s*-wave SC and CDW[81] that includes the phase fluctuations of both *s*-wave SC and CDW order parameters has demonstrated duality between the *s*-wave SC and CDW orders. Hence, quantum phase fluctuations between the vortices of *s*-wave SC and the dislocations of CDW can lead to gapless excitations. While effective theory can make qualitative justifications for the occurrence of gapless excitations, it does not provide quantitative spectroscopic information for direct comparison with experimental data. To investigate the effect of quantum phase fluctuations on the low-energy spectral characteristics in a coexisting *s*-wave SC and CDW system, we must include the self-energy ($\Sigma$) corrections associated with quantum phase fluctuations into the Green's function ($G_0$) of the mean-field Hamiltonian. Specifically, the total Green's function ($G$) after the self-energy correction is given by the Dyson's equation $G^{-1} = G_0^{-1} - \Sigma$, and the density of states can be obtained directly from $G$ by the following relation

$$N(E) = -\frac{1}{\pi}\,\mathrm{Im}\int d\xi_k\,\mathrm{Tr}\left[\hat{G}(\mathbf{k},E)\right]\cdot \tag{2}$$

Here the hat notation refers to the matrix representation of the Green's function. Specifically, in the case of coexisting *s*-wave SC and CDW, the Green's function must be expressed as (4×4) matrices in the basis of[76]

$$\left(c^{\dagger}_{\mathbf{k}\uparrow} \quad c_{-\mathbf{k}\downarrow} \quad c^{\dagger}_{\mathbf{k}+\mathbf{Q}\uparrow} \quad c_{-\mathbf{k}-\mathbf{Q}\downarrow}\right), \tag{3}$$

as does the self-energy correction. In the limit of a much weaker CDW potential relative to the SC pairing potential, $|V_0| << |\Delta_{SC}|$, we may restrict the self-energy correction $\Sigma = \Sigma_{SC} + \Sigma_{CDW}$ solely to that associated with the quantum phase fluctuations of the superconducting order parameter, $\Sigma \approx \Sigma_{SC}$. Thus, at low temperatures and in the absence of magnetic field, we obtain[82,83]

$$\begin{aligned}\Sigma_{SC}(\mathbf{k},E) &= \sum_{\mathbf{q}}\left[m\mathbf{v}_F(\mathbf{k})\right]_{\alpha}\left[m\mathbf{v}_F(\mathbf{k})\right]_{\beta}\left\langle v_s^{\alpha}(\mathbf{q})v_s^{\beta}(-\mathbf{q})\right\rangle_{\mathrm{ring}}\hat{G}(\mathbf{k}-\mathbf{q},E),\\ &= \Sigma^{l}_{SC}(\mathbf{k},E) + \Sigma^{t}_{SC}(\mathbf{k},E),\\ &= \sum_{\mathbf{q}}\left[m\mathbf{v}_F\cdot\hat{q}\right]^2 C_l(\mathbf{q})\hat{G}(\mathbf{k}-\mathbf{q},E) + \sum_{\mathbf{q}}\left[m\mathbf{v}_F\times\hat{q}\right]^2 C_t(\mathbf{q})\hat{G}(\mathbf{k}-\mathbf{q},E),\end{aligned} \tag{4}$$

where $\hat{G}$ is the full Green's function that contains the self-energy correction due to the SC quantum phase fluctuations, $C_l(\mathbf{q})$ and $C_t(\mathbf{q})$ are, respectively, the longitudinal and transverse components of the velocity-velocity correlation

function $\left\langle v_s^{\alpha}(\mathbf{q}) v_s^{\beta}(-\mathbf{q}) \right\rangle_{\text{ring}}$, with $\alpha$, $\beta$ denoting the velocity components and $\langle\rangle_{\text{ring}}$ referring to ring diagrams[82,83]. For the particular case of our interest at $T = 0$, we can ignore the transverse phase fluctuations, and the dominating quantum phase fluctuations are associated with the longitudinal velocity-velocity correlation functions, with the size of the quantum phase fluctuations determined by the ratio of the Coulomb energy of a Cooper pair to the plasma energy. Taking $\lim_{T\to 0} \Sigma_{SC} \simeq \Sigma_{SC}^{l}$ and using the basis given in EQ (3), the self-energy satisfies the following[83]:

$$\hat{\Sigma}_{SC}^{l}(\mathbf{k},\mathbf{Q}) = \begin{pmatrix} \Sigma_{11}(\mathbf{k}) & \Sigma_{12}(\mathbf{k}) & 0 & 0 \\ \Sigma_{21}(\mathbf{k}) & \Sigma_{22}(\mathbf{k}) & 0 & 0 \\ 0 & 0 & \Sigma_{33}(\mathbf{k},\mathbf{Q}) & \Sigma_{34}(\mathbf{k},\mathbf{Q}) \\ 0 & 0 & \Sigma_{43}(\mathbf{k},\mathbf{Q}) & \Sigma_{44}(\mathbf{k},\mathbf{Q}) \end{pmatrix}, \tag{5}$$

where $\Sigma_{33}(\mathbf{k},\mathbf{Q}) = \Sigma_{11}(\mathbf{k}+\mathbf{Q})$, $\Sigma_{34}(\mathbf{k},\mathbf{Q}) = \Sigma_{12}(\mathbf{k}+\mathbf{Q})$, $\Sigma_{43}(\mathbf{k},\mathbf{Q}) = \Sigma_{21}(\mathbf{k}+\mathbf{Q})$, and $\Sigma_{44}(\mathbf{k},\mathbf{Q}) = \Sigma_{22}(\mathbf{k}+\mathbf{Q})$. We may further simplify the Green's function expression by the following approximation:

$$\hat{G} = \hat{G}_0 + \hat{G}_0\hat{\Sigma}\hat{G} = \hat{G}_0 + \hat{G}_0\hat{\Sigma}\left(\hat{G}_0 + \hat{G}_0\hat{\Sigma}\hat{G}_0 + \cdots\right) \approx \hat{G}_0 + \hat{G}_0\hat{\Sigma}\hat{G}_0, \tag{6}$$

and obtain the excess density of states associated with the quantum phase fluctuations[83]:

$$\delta N(E) \approx -\frac{1}{\pi}\,\mathrm{Im}\int d\xi_k\,\mathrm{Tr}\left[\hat{G}_0\hat{\Sigma}\hat{G}_0\right] = -\frac{1}{\pi}\,\mathrm{Im}\left[\sum_k \left(G_{11}+G_{22}+G_{33}+G_{44}-G_{0,11}-G_{0,22}-G_{0,33}-G_{0,44}\right)\right]$$

$$= -\frac{1}{\pi}\,\mathrm{Im}\Big[G_{0,11}\left(\Sigma_{11}G_{0,11}+\Sigma_{12}G_{0,21}\right)+G_{0,12}\left(\Sigma_{21}G_{0,11}+\Sigma_{22}G_{0,21}\right)+G_{0,13}\left(\Sigma_{33}G_{0,31}+\Sigma_{34}G_{0,41}\right)+G_{0,14}\left(\Sigma_{43}G_{0,31}+\Sigma_{44}G_{0,41}\right)$$
$$+G_{0,21}\left(\Sigma_{11}G_{0,12}+\Sigma_{12}G_{0,22}\right)+G_{0,22}\left(\Sigma_{21}G_{0,12}+\Sigma_{22}G_{0,22}\right)+G_{0,23}\left(\Sigma_{33}G_{0,32}+\Sigma_{34}G_{0,42}\right)+G_{0,24}\left(\Sigma_{43}G_{0,32}+\Sigma_{44}G_{0,42}\right)$$
$$+G_{0,31}\left(\Sigma_{11}G_{0,13}+\Sigma_{12}G_{0,23}\right)+G_{0,32}\left(\Sigma_{21}G_{0,13}+\Sigma_{22}G_{0,23}\right)+G_{0,33}\left(\Sigma_{33}G_{0,33}+\Sigma_{34}G_{0,43}\right)+G_{0,34}\left(\Sigma_{43}G_{0,33}+\Sigma_{44}G_{0,43}\right)$$
$$+G_{0,41}\left(\Sigma_{11}G_{0,14}+\Sigma_{12}G_{0,24}\right)+G_{0,42}\left(\Sigma_{21}G_{0,14}+\Sigma_{22}G_{0,24}\right)+G_{0,43}\left(\Sigma_{33}G_{0,34}+\Sigma_{34}G_{0,42}\right)+G_{0,44}\left(\Sigma_{43}G_{0,34}+\Sigma_{44}G_{0,44}\right)\Big]. \tag{7}$$

Further numerical studies using EQs (2) -- (7) are underway to directly compare the theoretical calculations with experimental tunneling spectra of electron-type cuprates.

### 3.2 SDW or DDW as the relevant competing order in electron-doped cuprates with *s*-wave pairing symmetry

There has been much progress in the scanning tunneling spectroscopic studies of two-dimensional hole-type cuprates Bi-2212[13-16,18-20,45-47,84] and Na-CCOC[17]. The primary experimental findings include: low-temperature nano-scale spectral inhomogeneity at high quasiparticle energies ($|E| >\sim |\Delta_{SC}|$) for underdoped samples; robust low-energy ($|E| << |\Delta_{SC}|$) Bogoliubov quasiparticle characteristics for a wide range of doping levels at $T << T_c$; weakly momentum-dispersive and spatially checker-board like spectral modulations at high quasiparticle energies ($|E| > |\Delta_{SC}|$) for underdoped and optimally doped samples, which persist from $T << T_c$ to $T > T_c$; dichotomy in the quasiparticle coherence for underdoped samples even at low temperatures, with diminishing anti-nodal quasiparticle coherence at high energies ($|E| > |\Delta_{SC}|$); and field-induced checker-board like spectral modulations around vortices. These findings are strongly supportive of coexistence of competing order(s) with superconductivity. It might be tempting to attribute the checker-board like spectral modulations to CDW as the relevant competing order. However, empirically the checker-board like spectral modulations are generally very weak and are only noticeable at sufficiently large quasiparticle energies, which is a phenomenon fundamentally different from the observation of coexisting CDW and *s*-wave superconductivity in 2H-$NbSe_2$. Theoretically, the symmetry of CDW is not compatible with *d*-wave superconductivity, which would have favored CDW phase separation from SC rather than coexistence. On the other hand, spin-density wave (SDW)[7-9,55] and *d*-density wave (DDW, also known as orbital antiferromagnetism)[10] are possible competing orders associated with respectively the spin- and current-degrees of excitations around ($\pi$, $\pi$) in the momentum space. These competing orders can only couple with the charge channel via higher-order interactions and are therefore expected to give rise to substantially weaker effects than CDW on the quasiparticle spectra.

While both SDW and DDW are feasible competing orders that can account for various spectral characteristics in hole-type cuprates, there are also different experimental consequences associated with these two competing orders. For instance, DDW breaks the time-reversal symmetry[10] and therefore its coexistence with *d*-wave SC would generate time-reversal symmetry breaking components that in principle could be revealed directly in either the quasiparticle spectral characteristics or phase sensitive measurements of the superconductor. However, to date the majority of experimental data appears to be in favor of the absence of any broken time-reversal symmetry component.[30-35] On the other hand, quasiparticle spectra derived from both scanning tunneling spectroscopy and angular resolved photo emission spectroscopy (ARPES) seem to indicate that the bosonic excitations coupled with quasiparticles are primarily of the spin origin, and these excitations have energy scales comparable to those of the $(\pi, \pi)$ spin resonance and/or incommensurate spin fluctuations as determined from neutron scattering.[48,49] Theoretically, Green's function calculations based on the spin-fermion model for the cuprates have produced quasiparticle spectral characteristics consistent with experimental findings.[69-71] Our studies of the doping dependence of the satellite features in the quasiparticle tunneling spectra of Y-123 and the comparison of our data with those of the Bi-2212 are also consistent with the notion that bosonic excitations associated with the spin degrees of freedom are highly relevant to the spectral characteristics of cuprate superconductors. Thus, empirical findings to date seem to favor SDW over DDW as the relevant competing order for hole-type cuprates, although further experimental investigation is needed to verify the exact nature of the competing order. On the theoretical front, in contrast to the exact $SO(4)$ description[79,80] for coexistent CDW and *s*-wave SC, $SO(5)$ symmetry is only approximate for *d*-wave SC and SDW because $SO(5)$ symmetry applies to *d*-wave SC and antiferromagnetism (AFM),[7] whereas SDW are Goldstone modes of AFM that couples with the underlying crystalline lattice. Thus, to place SDW as the relevant competing order in hole-type cuprates on a sound theoretical foundation, one needs to generalize existing $SO(5)$ theory[7] to encompass coexistent SDW and *d*-wave SC and to verify the possibility of duality between SDW and *d*-wave SC. A larger symmetry group that incorporates both the $SO(5)$ group and the symmetry of the cuprate lattice structure may be necessary to fully account for the observation of spin fluctuations in hole-type cuprates.

### 3.3 Global symmetry and phase diagrams for the cuprates

The above discussion suggests that a complete theory for cuprate superconductivity must provide consistent descriptions for the interplay of competing orders and superconductivity as well as for the resulting physical phenomena. It seems natural to adapt a viewpoint that the physical phenomena of all cuprates may be described in terms of the elements of a global symmetry group, and various non-universal phenomena observed in different cuprates may simply be the result of different characteristics associated with different subgroups. By identifying the global symmetry of the cuprates, one can have a better understanding for the mechanism of symmetry breaking that leads to different phases in the ground state and the resultant low-energy excitations. Empirically, systematic studies of the physical properties of a variety of electron- and hole-type cuprates as a function of the doping level and the number of $CuO_2$ layers per unit cell will be imperative for identifying the nature of the relevant competing order(s) and the evolution of the competing order ($\Phi$) and superconductivity ($\Psi$) with varying temperature ($T$), magnetic field ($H$), and material parameters ($\alpha$). By systematic exploration of the phase diagrams of $\Psi$ and $\Phi$ for a wide variety of the cuprates as a function of $T$, $H$ and $\alpha$, we hope to eventually establish the global symmetry of all cuprates, whereby unraveling the microscopic mechanism for cuprate superconductivity.

## 4. SUMMARY

In this work we investigate the effect of competing orders on the microscopic low-energy excitations and macroscopic vortex state fluctuations in cuprate superconductors by means of low-temperature scanning tunneling spectroscopy and high-field magnetization measurements. Our preliminary experimental results on both electron- and hole-type cuprates suggest that cuprate superconductors are generally in close proximity to quantum criticality and exhibit strong quantum fluctuations due to the presence of competing orders in the ground state. We suggest that the presence of competing orders plays an important role in the extreme type-II nature and the strong vortex-state fluctuations of cuprate superconductors. We further examine the issue of whether the competing order is universal amongst different cuprates based on existing experimental and theoretical evidences, and suggest that CDW is likely the relevant competing order in electron-type cuprate superconductors of *s*-wave pairing symmetry, whereas SDW or DDW is more compatible with hole-type cuprate superconductors of predominant *d*-wave pairing symmetry. We propose to conduct more systematic

studies of the phase diagrams of a wide variety of cuprates as a function of temperature, magnetic field, doping level, disorder, and the number of the $CuO_2$ planes per unit cell, because information derived from these studies can help elucidate the global symmetry and the microscopic pairing mechanism of cuprate superconductivity.

## ACKNOWLEDGEMENT

The research at Caltech was jointly supported by the NSF Grant No. DMR-0103045, and the work at Pohang University was supported by the Ministry of Science and Technology of Korea through the Creative Research Initiative Program. We thank Professor Sudip Chakravarty and Professor Subir Sachdev for insightful discussions.

## REFERENCES

1. "Vortices in high-temperature superconductors", G. Blatter, M. V. Feigel'man, V. B. Geshkenbein, A. I. Larkin, and V. M. Vinokur, Rev. Mod. Phys. **66**, 1125 (1994).
2. "Effects of controlled static disorder on vortex dynamics of type-II superconductors -- A scaling approach", N.-C. Yeh, D. S. Reed, W. Jiang, U. Kriplani, D. A. Beam, M. Konczykowski, F. Holtzberg, and C. C. Tsuei, in Advances in Superconductivity -- VII, Vol.**1**, pg. 455--461, Spinger-Verlag, Tokyo (1995).
3. "Experimental investigations of the critical vortex dynamics in extreme type-II superconductors with controlled static disorder", N.-C. Yeh, W. Jiang, D. S. Reed, U. Kriplani, T. A. Tombrello, M. Konczykowski, F. Holtzberg, and C. C. Tsuei, in "Ferroelectrics", Gordon and Beach Science Publishers, Vol.**177**, 143 (1996).
4. "Lindemann criterion and vortex lattice phase transitions in type-II superconductors", J. Kierfeld and V. M. Vinokur, Phys. Rev. B **69**, 024501 (2004).
5. "Fluctuations and intrinsic pinning in layered superconductors", L. Balents and D. R. Nelson, Phys. Rev. Lett. **73**, 2618 (1994).
6. "Quantum smectic and supersolid order in helium films and vortex arrays", L. Balents and D. R. Nelson, Phys. Rev. B **52**, 12951 (1995).
7. "A unified theory based on SO(5) symmetry of superconductivity and antiferromagnetism", S.-C. Zhang, Science **275**, 1089 (1997).
8. "Competing orders and quantum criticality in doped antiferromagnets", M. Vojta, Y. Zhang, and S. Sachdev, Phys. Rev. B **62**, 6721 (2000).
9. "Order and quantum phase transitions in the cuprate superconductors", S. Sachdev, Rev. Mod. Phys. **75**, 913 (2003).
10. "Hidden order in cuprate superconductors", S. Chakravarty, R. B. Lauhlin, D. K. Morr and C. Nayak, Phys. Rev. B **63**, 094503 (2001).
11. "Recent Advances in High-Temperature Superconductivity", N.-C. Yeh, Highlight in Bulletin of Assoc. Asia Pacific Phys. Soc. **12**, 2 (2002); cond-mat/0210656.
12. "How to detect fluctuating stripes in the high-temperature superconductors", S. A. Kivelson, I. P. Bindloss, E. Fradkin, V. Organesyan, J. M. Tranquada, A. Kapitulnik, and C. Howald, Rev. Mod. Phys. **75**, 1201 (2003).
13. "Imaging quasiparticle interference in $Bi_2Sr_2CaCu_2O_{8+\delta}$", J. E. Hoffman, K. McElroy, D.-H. Lee, K. M. Lang, H. Eisaki, S. Uchida, and J. C. Davis, Science **297**, 1148 (2002).
14. "Relating atomic-scale electronic phenomena to wave-like quasiparticle states in superconducting $Bi_2Sr_2CaCu_2O_{8+\delta}$". K. McElroy, R. W. Simmonds, J. E. Hoffman, H. Eisaki, S. Uchida and J. C. Davis, Nature **422**, 592 (2003).
15. "Periodic density-of-states modulations in superconducting $Bi_2Sr_2CaCu_2O_{8+\delta}$", C. Howald, H. Eisaki, N. Kaneko, M. Greven and A. Kapitulnik, *Phys. Rev. B* **67**, 014533 (2003).
16. "Local ordering in the pseudogap state of the high-Tc superconductor $Bi_2Sr_2CaCu_2O_{8+\delta}$", M. Vershinin, S. Misra, S. Ono, Y. Abe, Y. Ando, and A. Yazdani, Science **303**, 1995 (2004).

17. “A `checkerboard’ electronic crystal state in lightly hole-doped $Ca_{2-x}Na_xCuO_2Cl_2$”, T. Hanaguri, C. Lupien, Y. Kohsaka, D.-H. Lee, M. Azuma, M. Takano, H. Takagi, and J. C. Davis, Nature **430**, 1001 (2004).
18. “Coincidence of checkerboard charge order and antinodal state decoherence in strongly underdoped $Bi_2Sr_2CaCu_2O_{8+\delta}$”, K. McElroy, D.-H. Lee, J. E. Hoffman, K. M. Lang, J. Lee, E. W. Hudson, H. Eisaki, S. Uchida and J. C. Davis, Phys. Rev. Lett. **94**, 197005 (2005).
19. “Quasiparticle scattering interference in high-temperature superconductors”, Q. H. Wang and D.-H. Lee, Phys. Rev. B **67**, 020511(R) (2003).
20. “Collective modes and quasiparticle interference on the local density of states of cuprate superconductors”, C.-T. Chen and N.-C. Yeh, Phys. Rev. B **68**, 220505(R) (2003).
21. “Destruction of the Fermi surface in underdoped high-$T_c$ superconductors”, M. R. Norman, H. Ding, M. Randeria, J. C. Campuzano, T. Yokoya, T. Takeuchi, T. Takahashi, T. Mochiku, K. Kadowaki, P. Guptasarma, and D. G. Hinks, Nature **392**, 157 (1998).
22. “Signature of superfluid density in the single-particle excitation spectrum of $Bi_2Sr_2CaCu_2O_{8+\delta}$”, D. L. Feng, D. H. Lu, K. M. Shen, C. Kim, H. Eisaki, A. Damascelli, R. Yoshizaki, J.-i. Shimoyama, K. Kishio, G. D. Gu, S. Oh, A. Andrus, J. O'Donnell, J. N. Eckstein, and Z.-X. Shen, Science **289**, 277 (2000).
23. “Coherent quasiparticle weight and its connection to high-$T_c$ superconductivity from angle-resolved photoemission”, H. Ding, J. R. Engelbrecht, Z. Wang, J. C. Campuzano, S.-C. Wang, H.-B. Yang, R. Rogan, T. Takahashi, K. Kadowaki, and D. G. Hinks, Phys. Rev. Lett. **87**, 227001 (2001).
24. “Metallic behavior of lightly doped $La_{2-x}Sr_xCuO_4$ with a Fermi surface forming an arc”, T. Yoshida, X. J. Zhou, T. Sasagawa, W. L. Yang, P. V. Bogdanov, A. Fujimori, H. Eisaki, Z.-X. Shen, T. Kakeshita, and S. Uchida, Phys. Rev. Lett. **91**, 027001 (2003).
25. “Dichotomy between nodal and antinodal quasiparticles in underdoped $(La_{2-x}Sr_x)CuO_4$ superconductors”, X. J. Zhou, T. Yoshida, D.-H. Lee, W. L. Yang, V. Brouet, F. Zhou, W. X. Ti, J. W. Xiong, Z. X. Zhou, T. Sasagawa, T. Kakeshita, H. Eisaki, S. Uchida, A. Fujimori, H. Hussain, and Z.-X. Shen, Phys. Rev. Lett. **92**, 187001 (2004).
26. “Scanning tunneling spectroscopic studies of cuprate superconductors”, N.-C. Yeh, C.-T. Chen, R. P. Vasquez, C. U. Jung, S. I. Lee, K. Yoshida, and S. Tajima, J. Low Temp. Phys. **131**, 435 (2003); cond-mat/0207594.
27. “Non-universal pairing symmetry and pseudogap phenomena in hole- and electron-doped cuprate superconductors”, N.-C. Yeh and C.-T. Chen, Int. J. Mod. Phys. B **17**, 3575 (2003); cond-mat/0302217.
28. “Strongly correlated s-wave superconductivity in the n-type infinite-layer cuprate”, C.-T. Chen, P. Seneor, N.-C. Yeh, R. P. Vasquez, L. D. Bell, C. U. Jung, J. Y. Kim, Min-Seok Park, Heon-Jung Kim, and Sung-Ik Lee, Phys. Rev. Lett. **88**, 227002 (2002).
29. “Gap anisotropy, spin fluctuations, and normal-state properties of the electron-doped superconductor $Sr_{0.9}La_{0.1}CuO_2$”, G. V. M. Williams, R. Dupree, A. Howes, S. Kramer, H. J. Trodahl, C. U. Jung, M.-S. Park, and S.-I. Lee, Phys. Rev. B **65**, 224520 (2002).
30. “Phase sensitive tests of the symmetry of the pairing state in the high-temperature superconductors -- evidence for $d_{x^2-y^2}$ symmetry”, D. J. van Harlingen, Rev. Mod. Phys. **67**, 515 (1995).
31. “Pairing symmetry in cuprate superconductors”, C. C. Tsuei and J. Kirtley, Rev. Mod. Phys. **72**, 969 (2000).
32. “Directional tunneling and Andreev reflection on $YBa_2Cu_3O_7$ single crystals: Predominance of d-wave pairing symmetry verified with the generalized BTK theory”, J. Y. T. Wei, N.-C. Yeh, D. F. Garrigus, and M. Strasik, Phys. Rev. Lett. **81**, 2542 (1998).
33. “Directional tunneling spectroscopy studies of the temperature and doping dependence of the pairing symmetry in cuprate superconductors”, N.-C. Yeh, J. Y. T. Wei, C.-T. Chen, W.-D. Si and X.-X. Xi, Physica C **341-348**, 1639 (2000).
34. “Spatial homogeneity and doping dependence of quasiparticle tunneling spectra in cuprate superconductors”, N.-C. Yeh, C.-T. Chen, G. Hammerl, J. Mannhart, S. Tajima, K. Yoshida, A. Schmehl, C. W. Schneider and R. R. Schulz, Physica C **364-365**, 450 (2001)

35. “Evidence of doping-dependent pairing symmetry in cuprate superconductors”, N.-C. Yeh, C.-T. Chen, G. Hammerl, J. Mannhart, A. Schmehl, C. W. Schneider, R. R. Schulz, S. Tajima, K. Yoshida, D. Garrigus, and M. Strasik, Phys. Rev. Lett. **87**, 087003 (2001).

36. “Investigating the pairing state of cuprate superconductors via quasiparticle tunneling and spin injection”, N.-C. Yeh, C.-T. Chen, C.-C. Fu, P. Seneor, Z. Huang, C. U. Jung, J. Y. Kim, Min-Seok Park, Heon-Jung Kim, S.-I. Lee, K. Yoshida, S. Tajima, G. Hammerl, and J. Mannhart, Physica C **367**, 174 (2002).

37. “Raman study of carrier-overdoping effects on the gap in high-$T_c$ superconducting cuprates”, T. Masiu, M. Limonov, H. Uchiyama, S. Lee, S. Tajima, and A. Yamanaka, Phys. Rev. B **68**, 060506(R) (2003).

38. “Substitution of Cu in the electron-doped infinite-layer superconductor $Sr_{0.9}La_{0.1}CuO_2$: Ni reduces $T_c$ faster than Zn”, C. U. Jung, J. Y. Kim, M. S. Park, M. S. Kim, H. J. Kim, S. Y. Lee and S. I. Lee, Phys. Rev. B **65,** 172501 (2002).

39. “Doping dependent pairing symmetry in n-type cuprates $Nd_{1.85}Ce_{0.15}CuO_{4-\delta}$”, J. A. Skinta *et al.*, Phys. Rev. Lett. **88**, 207005 (2002).

40. “Magnetic penetration depth measurements of $Pr_{1.85}Ce_{0.15}CuO_{4-\delta}$ films on buffered substrates: evidence for a nodeless gap”, M. S. Kim, J. A. Skinta, T. R. Lemberger, A. Tsukada, and M. Naito, Phys. Rev. Lett. **91,** 087001 (2003).

41. “Experimental investigation of the asymmetric spectroscopic characteristics of electron- and hole-doped cuprates”, N.-C. Yeh, C.-T. Chen, A. D. Beyer, C. R. Hughes, T. A. Corcovolis and S.-I. Lee, Physica C **408-410**, 792 (2004); [cond-mat/0405073].

42. “The pseudogap in high-temperature superconductors: an experimental survey”, T. Timusk and B. Statt, Rep. Prog. Phys. **62**, 61 (1999).

43. “Possible pseudogap behavior of electron-doped high-temperature superconductors”, S. Kleefisch, B. Welter, A. Marx, L. Alff, R. Gross and M. Naito, Phys. Rev. B **63**, 100507 (2001).

44. “A hidden pseudogap under the `dome’ of superconductivity in electron doped high-temperature superconductors”, L. Alff, Y. Krockenberger, B. Welter, M. Schonecke, R. Gross, D. Manske, and M. Naito, Nature **422**, 698 (2003).

45. “Microscopic electronic inhomogeneity in the high-$T_c$ superconductor $Bi_2Sr_2CaCu_2O_{8+\delta}$”, S. H. Pan, J. P. O’Neal, R. L. Badzey, C. Chamon, H. Ding, J. R. Engelbrecht, Z. Wang, H. Eisaki, S. Uchida, A. K. Gupta, K.-W. Ng, E. W. Hudson, K. M. Lang, and J. C. Davis, Nature **413**, 282 (2001).

46. “Inherent inhomogeneities in tunneling spectra of $Bi_2Sr_2CaCu_2O_{8-x}$ crystals in the superconducting state”, C. Howald, R. Fournier, and A. Kapitulnik, Phys. Rev. B **64**, 100504 (2001).

47. “Imaging the granular structures of high-$T_c$ superconductivity in underdoped $Bi_2Sr_2CaCu_2O_{8+\delta}$”, K. M. Lang, V. Madhavan, J. E. Hoffman, E. W. Hudson, H. Eisaki, S. Uchida, and J. C. Davis, Nature **415**, 412 (2002).

48. “Spin susceptibility in underdoped $YBa_2Cu_3O_{6+x}$”, H. F. Fong, P. Bourges, Y. Sidis, L. P. Regnault, J. Bossy, A. Ivanov, D. L. Milius, I. A. Aksay, and B. Keimer, Phys. Rev. B **61**, 14773 (2000).

49. “Evolution of the resonance and incommensurate spin fluctuations in superconducting $YBa_2Cu_3O_{6+x}$”, P. Dai, H. A. Mook, R. D. Hunt, and F. Dogan, Phys. Rev. B **63**, 054525 (2001).

50. “Commensurate spin dynamics in the superconducting state of an electron-doped cuprate superconductor”, K. Yamada, K. Kurahashi, T. Uefuji, M. Fujita, S. Park, S.-H. Lee, and Y. Endoh, Phys. Rev. Lett. **90**, 137004 (2003).

51. “Neutron scattering study on electron-hole doping symmetry of high-temperature superconductivity”, K. Yamada *et al.*, J. Phys. Chem. Solids **60**, 1025 (1999).

52. “Quasiparticle spectroscopy and high-field phase diagrams of cuprate superconductors – An investigation of competing orders and quantum criticality”, N.-C. Yeh, C.-T. Chen, V. S. Zapf, A. D. Beyer, C. R. Hughes, M.-S. Park, K.-H. Kim, and S.-I. Lee, Int. J. Mod. Phys. B **19**, 285 (2005); [cond-mat/0408100].

53. “Experimental investigation of the competing orders and quantum criticality in the hole- and electron-doped cuprate superconductors”, N.-C. Yeh, C.-T. Chen, V. S. Zapf, A. D. Beyer, C. R. Hughes, M.-S. Park, K.-H. Kim, and S.-I. Lee, Chinese J. Phys. **43** (2005); [cond-mat/0408105].

54. “Dimensionality of superconductivity and vortex dynamics in the infinite-layer cuprate $Sr_{0.9}M_{0.1}CuO_2$ (M = La, Gd)”, V. S. Zapf, N.-C. Yeh, A. D. Beyer, C. R. Hughes, C. H. Mielke, N. Harrison, M. S. Park, K. H. Kim, and S.-I. Lee, Phys. Rev. B **71**, 134526 (2005).

55. “Spin-ordering quantum transitions of superconductors in a magnetic field”, E. Demler, S. Sachdev and Y. Zhang, Phys. Rev. Lett. **87**, 067202 (2001).

56. “Thermal and disorder fluctuations in anisotropic superconducting $Nd_{1.85}Ce_{0.15}CuO_4$ epitaxial films”, N.-C. Yeh, W. Jiang, D. S. Reed, A. Gupta, F. Holtzberg, and A. Kussmaul, Phys. Rev. B **45**, 5710 (1992).

57. “Critical fluctuations and pinning effects on the vortex transport in superconducting $YBa_2Cu_3O_7$ single crystals”, N.-C. Yeh, W. Jiang, D. S. Reed, U. Kriplani, and F. Holtzberg, Phys. Rev. B **47**, 6146 (1993).

58. “Experimental determination of the B-T diagram of $YBa_2Cu_3O_{7-\delta}$ to 150 T for B $\perp$ c”, J. L. O'Brien, H. Nakagawa, A. S. Dzurak, R. G. Clark, B. E. Kane, N. E. Lumpkin, R. P. Starrett, N. Murira, E. E. Mitchell, J. D. Goettee, D. G. Rickel, and J. S. Brooks, Phys. Rev. B **61**, 1584 (2000).

59. “Null orbital frustration at the pseudogap boundary in a layered cuprate superconductor”, L. Krusin-Elbaum, T. Shibauchi, and C. H. Mielke, Phys. Rev. Lett. **92**, 097004 (2004).

60. “Evidence for coexistence of the superconducting gap and the pseudogap in Bi-2212 from intrinsic tunneling spectroscopy”, V. M. Krasnov, A. Yurgens, D. Winkler, P. Delsing, and T. Claeson, Phys. Rev. Lett. **84**, 5860 (2000).

61. “Synthesis ans pinning properties of the infinite-layer superconductor $Sr_{0.9}La_{0.1}CuO_2$”. C. U. Jung, J. Y. Kim, Mun-Seog Kim, Min-Seok Park, Heon-Jung Kim, Yushu Yao, S. Y. Lee, and S.-I. Lee, Physica C **366**, 299 (2002)., Physica C **366**, 299 (2002).

62. “Enhanced anisotropic nature of $HgBa_2Ca_3Cu_4O_{10+\delta}$”, M.-S. Kim, S.-I. Lee, S. C. Yu, I. Kuzemskaya, E. S. Itskevich, and K. A. Lokshin, Phys. Rev. B **57**, 6121 (1998).

63. “Two-dimensional nature of four-layer cuprate superconductors”, M.-S. Kim, C. U. Jung, S.-I. Lee and A. Iyo, Phys. Rev. B **63**, 134513 (2001).

64. “NMR study of carrier distribution and superconductivity in multilayered high-$T_c$ cuprates”, H. Kotegawa *et al.*, J. Phys. Chem. Solids **62**, 171 (2001).

65. “An explanation for a universality of transition temperatures in families of copper oxide superconductors”, S. Chakravarty, H.-Y. Kee and K. Volker, Nature **428**, 53 (2004).

66. “Superconducting properties and Fermi-surface topology of the quasi-two-dimensional organic superconductor lambda-(BETS)(2)GaCl4 (BETS bis(ethylene-dithio)tetraselenafulvalene)”, C. Mielke, J. Singleton, M. S. Nam, N. Harrison, C. C. Agosta, B. Fravel, and L. K. Montgomery, J. Phys.: Condens. Matter **13**, 8325 (2001).

67. “Small sample magnetometers for magnetic and resistive measurements at low temperatures”, J. S. Brooks, M. J. Naughton, Y. P. Ma, P. M. Chaikin, and R. V. Chamberlin, Rev. Sci. Inst. **59**, 117 (1987).

68. “Cantilever magnetometry in pulsed magnetic fields”, M. J. Naughton, P. Ulmet, A. Narjis, S. Askenazy, M. V. Chaparala, and A. P. Hope, Rev. Sci. Inst. **68**, 4061 (1997).

69. “A relation between the resonance neutron peak and ARPES data in cuprates”, Ar. Abanov and A. V. Chubukov, Phys. Rev. Lett. **83**, 1652 (1999);

70. “Relative positions of the 2$\Delta$ peaks in Raman and tunneling spectra of d-wave superconductors”, A. V. Chubukov, and N. Gemelke, Phys. Rev. B **61**, R6467 (2000).

71. “Effects of spin fluctuations on the tunneling spectroscopy in high-$T_c$ superconductors”, C. L. Wu, C. Y. Mou and D. Chang, Phys. Rev. B **63**, 172503 (2001).

72. “The parent structure of the layered high-temperature superconductors”, T. Siegrist, S. M. Zahurak, D. W. Murphy, and R. S. Roth, Nature **334**, 231 (1988).

73. “Structure of superconducting $Sr_{0.9}La_{0.1}CuO_2$ ($T_c$ = 42 K) from neutron powder diffraction”, J. D. Jorgensen *et al.*, Phys. Rev. B **47**, 14654 (1993).

74. “High-pressure synthesis of the homogeneous infinite-layer superconductor $Sr_{0.9}La_{0.1}CuO_2$”, C. U. Jung *et al.*, Physica C **364,** 225 (2001).

75. “Anisotropy and reversible magnetization of the infinite-layer superconductor $Sr_{0.9}La_{0.1}CuO_2$”, M.-S. Kim, T. R. Lemberger, C. U. Jung, J. H. Choi, J. Y. Kim, H. J. Kim, and S. I. Lee, *Phys. Rev. B* **66**, 214509 (2002).
76. “Impurity and fluctuation effects in charge-density-wave superconductors”, G. S. Grest, K. Levin and M. J. Nass, Phys. Rev. B **25**, 4562 (1982).
77. “Charge density wave and superconductivity in anisotropic materials”, K. Machida, J. Phys. Soc. Japan **53**, 712 (1984).
78. “Evidence for a connection between charge density waves and pressure enhancement of superconductivity in 2H-$NbSe_2$”, C. Berthier, P. Molinie and D. Jerome, Solid State Comm. **18**, 1393 (1976); D. Jerome, C. Berthier, P. Molinie and J. Rouvel, J. Phys. (Paris) **4**, 125 (1976).
79. “η pairing and off-diagonal long-range order in a Hubbard model”, C. N. Yang, Phys. Rev. Lett. **63**, 2144 (1989).
80. “SO4 symmetry in a Hubbard model”, C. N. Yang and S. C. Zhang, Mod. Phys. Lett. B **4**, 759 (1990).
81. “Duality between unidirectional charge-density-wave order and superconductivity”, D.-H. Lee, Phys. Rev. Lett. **88**, 227003 (2002).
82. “Effect of phase fluctuations on the single-particle properties of underdoped cuprates”, H.-J. Kwon and A. T. Dorsey, Phys. Rev. B **59**, 6438 (1999).
83. “Competing orders and quantum phase fluctuations on the low-energy excitation spectra of cuprate superconductors”, C.-T. Chen and N.-C. Yeh, to be published.
84. “A four unit cell periodic pattern of quasi-particle states surrounding vortex cores in $Bi_2Sr_2CaCu_2O_{8+\delta}$”, J. E. Hoffman, E. W. Hudson, K. M. Lang, V. Madhavan, H. Eisaki, S. Uchida, and J. C. Davis, Science **295**, 466 (2002).